On Numerical Investigation of Buckling in Two-Directional Porous Functionally Graded Beam Using Higher Order Shear Deformation Theory

P. Bridjesh [a]*, N.K. Geetha [b], G.C.M. Reddy [a]

[a] Department of Mechanical Engineering, MLR Institute of Technology, Hyderabad, 500049, India
[b] Department of Mathematics, Dayananda Sagar College of Engineering, Bengaluru, 560078, India

ABSTRACT

In functionally graded materials (FGM), pores have a key impact. A variety of properties, such as resistance to mechanical shock, thermal insulation, catalytic efficiency, and the release of thermal stress, can be added by gradually changing pores distribution from the inner surface to the exterior surface. Tensile strength and the material's Young's modulus are impacted by the level and distribution of porosity. Two directional functionally graded beams are subjected to different sets of boundary conditions by employing a fifth-order shear deformation theory. The power-law distribution shows that the material properties of the beam change in both axial and thickness directions. Axial and transverse cross-sectional deflections are given in polynomial forms in order to calculate the critical buckling load. The auxiliary functions are combined with the displacement functions to fulfill the boundary criteria. Considerations for the boundary conditions include the following three: Clamped - clamped (CC), Simply supported (SS), and Clamped-free (CF). The computed findings are contrasted with earlier attempts in order to aid in the convergence and verification investigations. The effects of different aspect ratios, boundary conditions, and gradient indices on the buckling responses of the two directional functionally graded beams are all investigated.

1. Introduction

New generation materials have been developed using improvements in material manufacturing methods to suit the need for use. Each period saw the innovation of particular materials to support the development of technology. Composite materials are made of two or more different materials yet nonetheless possess the necessary properties for a particular application [1]. However, the differences in mechanical properties at the interface of these two different materials can lead to significant interlaminar stresses [2]. Therefore, concerns with delamination and de-bonding will manifest in a hot environment. In general, for many years, isotropic homogenous materials of various types, such as those from the metal and polymer groups, have been widely used in a variety of technical fields [3]. The metal group of materials excels in great strength and toughness, whereas polymers excel in high flexibility as well as corrosion resistance. However, at extremely high temperatures, these materials are unable to withstand stresses [4]. Therefore, materials from the ceramics family could be used to combine these metals with polymers to benefit from their special qualities and improve properties such as thermal resistance [5]. A new variety of materials must be developed in order to accommodate the recent rise in the use of materials for engineering constructions that are subjected to heavy mechanical loads in hot conditions [6].

Progressive materials with mechanical qualities that change in space are called functionally graded materials (FGM). Components of FGM are made to vary constantly and smoothly in all gradient directions [7]. The main objective of FGM research is to create materials that can survive extremely high

---

temperatures so that ceramics can be mixed with other materials to form refractories, which are materials with remarkable heat resistance [8]. However, it is impossible to use ceramics to build engineering structures that can withstand significant mechanical stress. This could be due to the fact that ceramics have poor toughness properties, necessitating the mixing of ceramics with other materials such as metals and polymers that have strong toughness capabilities [9]. The transport industry, optics, energy storage, and conversion systems, semiconductors, the production of cutting tools and machine components, biosystems, etc. are just a few of the significant applications that the FGM could be employed. FGM could be available to address the issue and fulfill the requirement because certain applications call for specific key concerns 10].

Understanding how FGM structures react when exposed to static and dynamic loading conditions is essential for structural designs. To improve the predictability of how FGM structures would respond to different mechanical loads, numerous theories were proposed [11]. To analyze bending, buckling, and vibration in FGMs, several researchers have previously made specific theoretical and experimentally validated choices. Numerous techniques are used to explain the gradient of FGM that are constructed from two distinct phases of material [12]. In general, volume fraction distributions rather than actually graded microstructures are used to construct the bulk of approaches. Classical beam theory (CBT), developed by Bernoulli and Euler, is the simplest beam theory to analyze thin beams [13]. However, this approach is inappropriate for the investigation of thick Functionally Graded (FG) beams since it disregards the shear deformation impact. The displacements and stresses in thick beams are overestimated by CBT. The variation in the first order in axial displacement is an assumption made by Timoshenko in his 1921 theory. As a result, it is often referred to as first-order shear deformation theory (FSDT) or Timoshenko beam theory (TBT) [14]. The criterion for zero transverse shear stress could not be met on the top and bottom surfaces of the beam via FSDT. The strain energy brought on by the shear deformation effect must be properly taken into consideration to avoid the use of the shear correction factor. As a result, various scholars provide higher-order shear deformation theories to precisely predict the bending response. Sayyad and Ghugal [15] have provided a comprehensive analysis.

A substance is referred to as porous if it has pores that permit fluid to move through them. A porous substance's porosity is one of its key characteristics [16]. Permeability, tensile strength, and electrical conductivity are all influenced by the properties of the matrix and the fluid that fills the pores. Porous structures are frequently used in several fields, including civil engineering, marine engineering, and aerospace engineering. Recently, researchers have begun to pay more attention to functionally graded porous materials (FGPMs) [17].

FGPMs, in which the mechanical properties change continuously throughout the structure. These are substances whose porosity gradually changes over the course of their volume. The foundation material contains pores with varying porosity distribution. Porosity variation may be caused by modifications in pore density or size. Depending on the cell structure, FGPMs may be configured as open or closed cells [18]. Open-cell structures feature pores that are connected, whereas closed-cell structures have a substance that surrounds and isolates each cell. Through a gradual change in porosity, desirable qualities can be imparted.

Magnucki [19] looked at different types of buckling in porous beams with different properties. They assessed how porosity affected the strength as well as buckling load shear deformation theory and calculated the critical load. Magnucka-Blandzi [20], who also identified the appropriate dimensionless parameters to raise a critical force and lower beam mass, effectively developed a sandwich beam with an FG metal foam core. Using analytical solutions and the Euler-Bernoulli theory, Mojahedin et al [21], estimation of free vibration in FG thin beams with pores was made. Babaei et al. used the finite element approach to examine buckling, static, and dynamic [22] evaluations of an FG-saturated porous thick beam in accordance with higher-order beam theory. Mojahedin et al. [23] provided a solution for thermos-elastic analysis of a saturated FG porous beam by adapting the Timoshenko beam theory. In light of various beam theories and Navier's solution, Hung et al. [24] explored the static behavior of an FG sandwich beam with a fluid-infiltrating porous core. From the current literature, it can be concluded that the accuracy-based fifth-order shear deformation theory is not used to explore the impact of porosity on FGM beams.

The major focus of this paper is the critical buckling analysis of two-dimensional FG beams using Power Law variations in boundary conditions, aspect ratios, gradient indices, and porosity indices. A unique shear shape function is created to attain zero shear stress conditions at the top and lower surfaces of the FG beam, and the fifth-order theory is adjusted to take into consideration the effects of transverse shear deformation

2. Formulation and Mathematics

2.1. Formulation of Porous FG beam

The coordinate system for the beam used in the present research is presented in Figure 1. A rectangular FG beam with dimensions of length (L) in the x-direction, width (B) in the y-direction, and thickness (h) in the z-direction. It is assumed that material qualities differ continuously across the length, and thickness, directions. By grading the ceramic and metal phases, an FG rectangular beam in the thickness direction is produced. Here, the lower surface (z= -h/2) is made of metal and the upper surface (z= +h/2) is made of ceramic. The reference surface, or (z=0), is the central surface of the beam. Origin (O) is the midpoint of a rectangular beam (x,y), thus z = [-h/2, h/2]
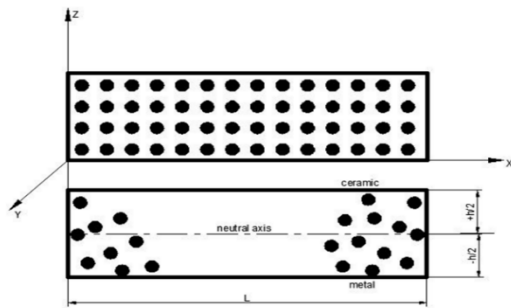

Fig. 1. Functionally graded beam geometry

The volume proportion of the component materials affects the material properties of the FG beam. It is anticipated that the thickness coordinate and material properties will work together. Porous volume fraction (Vf), as indicated in Eq. 1 [25], could be represented by the Power Law distribution in x and z.

$$V_f(x,z) = \left(\frac{z}{h} + \frac{1}{2}\right)^{P_z} \left(\frac{x}{L} + \frac{1}{2}\right)^{P_x} \tag{1}$$

here, P_z and P_x denote the behaviour of volume fraction throughout the thickness and length of the beam. Variation of porous volume fractions of ceramic in thickness and length directions is depicted in Figure 2.
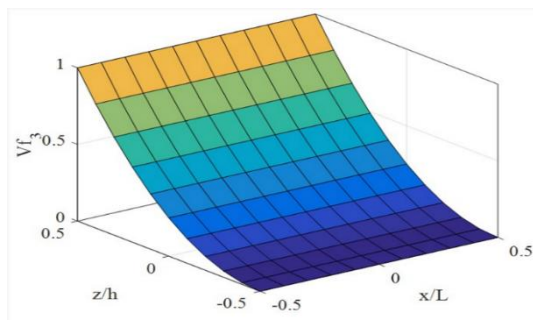

Fig. 2. Porous volume fraction of ceramic in thickness (z/h) and length (x/L) direction

Effective material properties in evenly distributed porous FG beams (P) can then be expressed as,

$$P(x,z) = (P_c - P_m)\left(\frac{z}{h} + \frac{1}{2}\right)^{P_z}\left(\frac{x}{L} + \frac{1}{2}\right)^{P_x}$$
$$+P_m - \frac{\alpha}{2}(P_c + P_m) \tag{2}$$

where α represents the coefficient of porosity (0≤α≤1), m and c represent the metal and ceramic phases.

As per the aforementioned relationship, Young's modulus (E), and mass density (ρ), which are used for material stiffness and moment of inertia estimation for evenly distributed porous FG beams can be expressed as:

$$E(x,z) = (E_c - E_m)\left(\frac{z}{h} + \frac{1}{2}\right)^{P_z}\left(\frac{x}{L} + \frac{1}{2}\right)^{P_x}$$
$$+E_m - \frac{\alpha}{2}(E_c + E_m) \tag{2a}$$

$$\rho(x,z) = (\rho_c - \rho_m)\left(\frac{z}{h} + \frac{1}{2}\right)^{P_z}\left(\frac{x}{L} + \frac{1}{2}\right)^{P_x}$$
$$+\rho_m - \frac{\alpha}{2}(\rho_c + \rho_m) \tag{2b}$$

Although there is a slight variance in Poisson's ratio value as compared with other properties, it is considered to be constant because computations are made using the average value.

Likewise, the effective material properties of unevenly distributed porous FG beams (P) can then be expressed as,

$$P(x,z) = (P_c - P_m)\left(\frac{z}{h} + \frac{1}{2}\right)^{P_z}\left(\frac{x}{L} + \frac{1}{2}\right)^{P_x}$$
$$+P_m - \frac{\alpha}{2}(P_c + P_m)\left(1 - \frac{2/z}{h}\right) \tag{3}$$

Young's modulus (E), and mass density (ρ) for unevenly distributed porous FG beams could be expressed as:

$$E(x,z) = (E_c - E_m)\left(\frac{z}{h} + \frac{1}{2}\right)^{P_z}\left(\frac{x}{L} + \frac{1}{2}\right)^{P_x}$$
$$+E_m - \frac{\alpha}{2}(E_c + E_m)\left(1 - \frac{2/z}{h}\right) \tag{3a}$$

and

$$\rho(x,z) = (\rho_c - \rho_m)\left(\frac{z}{h} + \frac{1}{2}\right)^{P_z}\left(\frac{x}{L} + \frac{1}{2}\right)^{P_x}$$
$$+\rho_m - \frac{\alpha}{2}(\rho_c + \rho_m)\left(1 - \frac{2/z}{h}\right) \tag{3b}$$

2.2. Constitute Equations for Displacement Field

For robust constructions and to save production costs, FG beams and plates that are subject to static and dynamic loads must be well-designed. When analyzing FGM constructions made by adapting classical beam and plate theories, the deflection findings of bending analysis are often found to be underestimated; nevertheless, critical loads and natural frequencies are typically overstated. In order to improve forecast accuracy, it is advisable to use theories that consider the effects of shear deformation while analyzing beams and plates formed by FGMs. To determine the impact of transverse shear and normal strain, Reddy's advanced higher-order shear deformation theory is modified. These are the displacement field and constitutive equations:

$$U(x,z,t) = u_0(x,t) + z\emptyset(x,t)$$
$$-f(z)\left(\emptyset(x,t) + \frac{\partial w_0}{\partial x}(x,t)\right) \tag{4a}$$

$$W(x,z,t) = w_0(x,t) \tag{4b}$$

where U is axial displacement and W is transverse displacement. u_0 and w_0 are the axial displacement at a given point on the neutral axis. $\frac{\partial w_0}{\partial x}$ is the bending slope and $\emptyset$ is the shear slope.

The displacement field equation in matrix form can be expressed as,

$$\binom{U}{W} = \begin{bmatrix} 1 & 0 & -z \\ 0 & 1 & 0 \end{bmatrix} \{u_0 \quad w_0 \quad w_{0,x}\}^T \tag{5}$$
$$= [z_d]\{d\}$$

The shape function f(z) could be used to determine transverse shear deformation and the non-zero strain field equations can be computed using Eqs. (4a) and (4b) as,

$$\varepsilon_x = \frac{\partial U}{\partial x} = \frac{\partial u_0}{\partial x} - z\frac{\partial^2 w_0}{\partial x^2}$$
$$+ f(z)\left(\frac{\partial \emptyset}{\partial x} + \frac{\partial^2 w_0}{\partial x^2}\right) \tag{6a}$$

$$\varepsilon_z = \frac{\partial W}{\partial z} = 0 \tag{6b}$$

$$\gamma_{xz} = f'\left[\emptyset + \frac{\partial w_0}{\partial x}\right] \tag{6c}$$

and

$$f(z) = \frac{h}{\pi} * sin\left[\frac{\pi * z}{h}\right]$$
$$- \frac{z}{\pi * n}\left(1 - \frac{1}{n} * \frac{2^{n-1}}{h} * z^{n-1}\right) \tag{7a}$$

$$f'(z) = \frac{h}{\pi} * sin\left[\frac{\pi}{h}\right]$$
$$- \frac{1}{\pi * n}\left(1 - \frac{1}{n} * \frac{2^{n-1}}{h} * (n-1)z^{n-2}\right) \tag{7b}$$

According to Hooke's Law and using Eqs. 6a, 6b, 6c, 7a, 7b, the field equations for stress can be deduced as follows:

$$\sigma_x = \frac{E(x,z)}{1 - \mu^2}\varepsilon_x \tag{8a}$$

$$\tau_{xz} = \frac{E(x,z)}{2(1 + \mu)}\gamma_{xz} \tag{8b}$$

2.3. Buckling Formulation in FG Beam

The Bi-directional FG beam's strain energy can be expressed as:

$$U = \frac{1}{2}\int_0^L \int_{\frac{-h}{2}}^{\frac{+h}{2}} (\sigma_x\varepsilon_x + \tau_{xz}\gamma_{xz})dzdx \tag{9}$$

Substituting Eqs. 6a, Eq. 6c, Eq. 8a, and Eq. 8b in Eq. 9, the obtained strain energy can be expressed as,

$$U = \frac{1}{2}\int_0^L \int_{\frac{-h}{2}}^{\frac{+h}{2}} \left(\frac{E(x,z)}{1-\mu^2}\varepsilon_x\varepsilon_x \right.$$
$$\left. + \frac{E(x,z)}{2(1+\mu)}\gamma_{xz}\gamma_{xz}\right)dzdx \tag{10}$$

$$U = \frac{1}{2}\int_0^L \int_{\frac{-h}{2}}^{\frac{+h}{2}} \left[\left(\frac{E(x,z)}{1-\mu^2}\left(\left(\frac{\partial u_0}{\partial x}\right)^2 \right.\right.\right.$$
$$+ \frac{\partial u_0}{\partial x}\frac{\partial^2 w_0}{\partial x^2}(2f - 2z)$$
$$+ \frac{\partial u_0}{\partial x}\frac{\partial \emptyset}{\partial x}(2f)$$
$$+ \left(\left(\frac{d^2 w_0}{dx^2}\right)^2\right)(z^2 - 2zf$$
$$\left. + f^2\right) + \frac{\partial^2 w_0}{\partial x^2}\frac{\partial \emptyset}{\partial x}(2f^2 \tag{11}$$
$$\left. - 2zf + \left(\frac{\partial \emptyset}{\partial x}\right)^2 (f)^2\right)$$
$$+ \frac{E(x,z)}{2(1+\mu)}\left(\emptyset^2(f')^2 \right.$$
$$+ \emptyset\frac{\partial w_0}{\partial x}(2f'^2)$$
$$\left.\left.\left. + \left(\left(\frac{d^2 w_0}{dx^2}(f')^2\right)\right)\right)\right]dzdx$$

Total strain energy and potential work are added to determine the beam's total potential energy (π).

$$\pi = U + V \tag{12}$$

$$u(x,t) = \sum_{j=1}^{m} A_j\theta_j(x)e^{i\omega t},$$

$$\theta_j(x) = \left(x + \frac{L}{2}\right)^{p_u}\left(x - \frac{L}{2}\right)^{q_u}x^{m-1} \tag{13}$$

$$w(x,t) = \sum_{j=1}^{m} B_j\varphi_j(x)e^{i\omega t},$$

$$\varphi_j(x) = \left(x + \frac{L}{2}\right)^{p_w}\left(x - \frac{L}{2}\right)^{q_w}x^{m-1} \tag{14}$$

$$\phi(x,t) = \sum_{j=1}^{m} C_j\psi_j(x)e^{i\omega t},$$

$$\psi_j(x) = \left(x + \frac{L}{2}\right)^{p_\phi}\left(x - \frac{L}{2}\right)^{q_\phi}x^{m-1} \tag{15}$$

The boundary conditions proposed are $\theta_j(x)$, $\varphi_j(x)$ and $\psi_j(x)$ and $\boldsymbol{\omega}$, the natural frequency of the beam. Unknown coefficients A_j, B_j, and C_j could be estimated using the complex number, $i = \sqrt{-1}$.

Substituting Eq. 14, and Eq. 15 in Eq. 13, and adapting the principle of minimum potential energy, we get,

$$\frac{\partial \Pi}{\partial A_j} = 0, \frac{\partial \Pi}{\partial B_j} = 0, \frac{\partial \Pi}{\partial C_j} = 0; \; j = 1,2,3,\ldots,m \tag{16}$$

The values of A_j, B_j, and C_j represented with q_j, can be used to estimate critical buckling loads for a two-dimensional FG beam as given in Eq. 17,

$$\left(\begin{bmatrix} [S_{11}] & [S_{12}] & [S_{13}] \\ [S_{12}]^T & [S_{22}] & [S_{23}] \\ [S_{13}]^T & [S_{23}]^T & [S_{33}] \end{bmatrix} - N_{cr}\begin{bmatrix} [0] & [0] & [0] \\ [0] & [K_{N0}] & [0] \\ [0] & [0] & [0] \end{bmatrix}\right)$$
$$\times \begin{Bmatrix} A \\ B \\ C \end{Bmatrix} = \begin{Bmatrix} \{0\} \\ \{0\} \\ \{0\} \end{Bmatrix} \tag{17}$$

The geometric stiffness and stiffness matrices are $[K_{N0}]$, and [Ski] and their components are given by,

$$S_{11}(i,j) = \int_{-L/2}^{L/2}\frac{E(x,z)}{1-\mu^2}\left[\left(x + \frac{L}{2}\right)^{p\theta}\left(x\right.\right.$$
$$\left.- \frac{L}{2}\right)^{q\theta}x^{i-1}\left(x + \frac{L}{2}\right)^{p\theta}\left(x\right. \tag{18}$$
$$\left.\left.- \frac{L}{2}\right)^{q\theta}x^{j-1}\right]dzdx$$

$$S_{12}(i,j) = (f - z)\int_{-L/2}^{L/2}\frac{E(x,z)}{1-\mu^2}\left[\left(x\right.\right.$$
$$\left.+ \frac{L}{2}\right)^{p\theta}\left(x - \frac{L}{2}\right)^{q\theta}x^{i-1}\left(x\right.$$
$$\left.+ \frac{L}{2}\right)^{p\varphi}\left(x\right. \tag{19}$$
$$\left.\left.- \frac{L}{2}\right)^{q\varphi}x, x^{j-1}\right]dzdx$$

$$S_{13}(i,j) = f\int_{-\frac{L}{2}}^{\frac{L}{2}}\frac{E(x,z)}{1-\mu^2}\times$$
$$\left[\left(x + \frac{L}{2}\right)^{p\theta}\left(x - \frac{L}{2}\right)^{q\theta}x^{i-1}\left(x + \frac{L}{2}\right)^{p\psi}\left(x\right.\right. \tag{20}$$
$$\left.\left.- \frac{L}{2}\right)^{q\psi}x^{j-1}\right]dzdx$$

$$S_{22}(i,j) = (z^2 - zf + f^2)\int_{-\frac{L}{2}}^{\frac{L}{2}}\frac{E(x,z)}{1-\mu^2}\times$$
$$\left[\left(x + \frac{L}{2}\right)^{p\varphi}\left(x - \frac{L}{2}\right)^{q\varphi}x, x^{i-1}\left(x + \frac{L}{2}\right)^{p\varphi}\left(x\right.\right.$$
$$\left.\left.- \frac{L}{2}\right)^{q\varphi}x, x^{j-1}\right]dzdx +$$
$$(f')^2\int_{-\frac{L}{2}}^{\frac{L}{2}}\frac{E(x,z)}{2(1+\mu)}\left[\left(x + \frac{L}{2}\right)^{p\varphi}\left(x\right.\right. \tag{21}$$
$$\left.- \frac{L}{2}\right)^{q\varphi}x, x^{i-1}\left(x + \frac{L}{2}\right)^{p\varphi}\left(x\right.$$
$$\left.\left.- \frac{L}{2}\right)^{q\varphi}x, x^{j-1}\right]dzdx$$

$$S_{23}(i,j) = (f^2 - zf)\int_{-\frac{L}{2}}^{\frac{L}{2}}\frac{E(x,z)}{1-\mu^2}\times$$
$$\left[\left(x + \frac{L}{2}\right)^{p\varphi}\left(x - \frac{L}{2}\right)^{q\varphi}x, x^{i-1}\left(x + \frac{L}{2}\right)^{p\psi}\left(x\right.\right.$$
$$\left.\left.- \frac{L}{2}\right)^{q\psi}x^{j-1}\right]dzdx +$$
$$(f')^2\int_{-\frac{L}{2}}^{\frac{L}{2}}\frac{E(x,z)}{2(1+\mu)}\left[\left(x + \frac{L}{2}\right)^{p\varphi}\left(x\right.\right. \tag{22}$$
$$\left.- \frac{L}{2}\right)^{q\varphi}x^{i-1}\left(x + \frac{L}{2}\right)^{p\psi}\left(x\right.$$
$$\left.\left.- \frac{L}{2}\right)^{q\psi}\right]dzdx$$

$$S_{33}(i,j) = (f)^2 \int_{-\frac{L}{2}}^{\frac{L}{2}} \frac{E(x,z)}{1-\mu^2} \times$$

$$\left[\left(x+\frac{L}{2}\right)^{p\psi} \left(x-\frac{L}{2}\right)^{q\psi} x^{i-1} \left(x+\frac{L}{2}\right)^{p\psi} \left(x - \frac{L}{2}\right)^{q\psi} x^{j-1} \right] + \qquad (23)$$

$$(f')^2 \int_{-\frac{L}{2}}^{\frac{L}{2}} \frac{E(x,z)}{2(1+\mu)} \left[\left(x+\frac{L}{2}\right)^{p\psi} \left(x-\frac{L}{2}\right)^{q\psi} \left(x + \frac{L}{2}\right)^{p\psi} \left(x - \frac{L}{2}\right)^{q\psi} \right] dz dx$$

$$K_{N0}(i,j) = \int_{-L/2}^{L/2} \left[\left(x+\frac{L}{2}\right)^{p\varphi} \left(x - \frac{L}{2}\right)^{q\varphi} x, x^{i-1} \left(x+\frac{L}{2}\right)^{p\varphi} \left(x - \frac{L}{2}\right)^{q\varphi} x, x^{j-1} \right] dz dx \quad (24)$$

2.4. Position of the Neutral Axis

According to the physical neutral surface concept [26], the physical neutral axis of the FG beam is given by:

$$z_0 = \frac{\int_{-\frac{h}{2}}^{\frac{h}{2}} z E(z) dz}{\int_{-\frac{h}{2}}^{\frac{h}{2}} E(z) dz} = \frac{(E_c - E_m)hp}{2(2+p)(E_c + E_m p)} \qquad (25)$$

It is clear that in a homogeneous isotropic beam, the geometric middle surface and the physical neutral surface are identical. The variation of the Power Law index on the position of the neutral axis is presented in Figure 3.
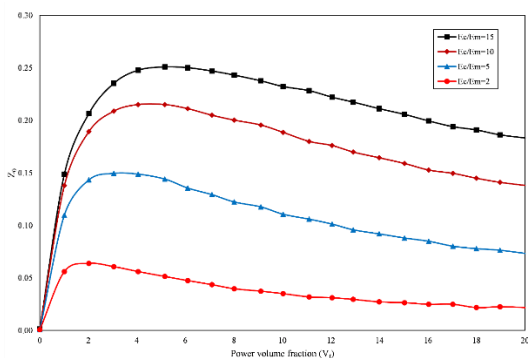

Fig. 3. Variation of Power Law index on the position of the neutral axis

3. Numerical Computation – Results and Discussion

The accuracy of the current approach is examined using several numerical examples,

including the impacts of gradient indexes i.e., material composition, on the buckling behaviour of two-dimensional FG beams, boundary conditions, and aspect ratios (L/h) have also been studied. Material properties of the constituents of the considered FG beam are as follows:

Alumina: Ec=380 GPa, ρc=3960 kg/m3, μc=0.3

Aluminium: Em=70 GPa, ρm=2702 kg/m3, μm=0.3

To analyze the shear deformation, the height of the beam is varied. Three varied boundary conditions, such as SS, CF, and CC are applied and tabulated in Table 1.

Table 1. Boundary conditions for the FG beam

Boundary condition	x= -L/2	x= L/2
SS	u=0, w=0	w=0
CF	u=0, w=0, ϕ=0, w'=0	
CC	u=0, w=0, ϕ=0, w'=0	u=0, w=0, ϕ=0, w'=0

The FG beam material properties fluctuate in the axial (L) and thickness direction (h), governed by the Power Law. Non-dimensional buckling load parameter, ($\bar{N}$cr) could be used for the representation of results. where,

$$\bar{N}\text{cr} = \frac{12 N_{cr} L^2}{E_2 b h^3} \qquad (26)$$

A homogeneous beam is taken into account for the convergence and verification investigations, and displacement functions with various numbers of terms (m=2, 4, 6, 8, 10, and 12) are used [27].

The calculated findings are provided as a dimensionless critical buckling load taking into account different gradient indices in both directions, aspect ratios, and boundary conditions, specifically SS, CC, and CF.

For comparison, the findings from the earlier investigations [25] in terms of dimensionless critical buckling load are utilized as presented in Table 2.

Table 2 shows that the results for the buckling behavior of SS and CF beams quickly converge since the displacement function has six terms. However, by employing 6 terms in the displacement function, the agreed findings of the CC boundary condition are obtained. To ensure accuracy, 12 terms from the polynomial expansion are employed for the complete buckling analysis of two directional FG beams [28].

Table 2. Critical buckling load of FGM beams with respect to various boundary conditions and aspect ratio (L/h) change

L/h	Theory		Boundary Conditions		
			SS	CC	CF
5	[25]		57.925	158.936	13.156
	Present	2 terms	58.427	159.438	13.658
		4 terms	49.123	154.538	13.562
		6 terms	49.098	152.649	13.561
		8 terms	49.098	152.649	13.561
		10 terms	49.098	152.649	13.561
		12 terms	49.098	152.649	13.561
20	[25]		63.148	223.944	13.474
	Present	2 terms	63.937	224.733	14.263
		4 terms	54.053	212.887	14.194
		6 terms	54.026	209.741	14.162
		8 terms	54.026	209.741	14.162
		10 terms	54.026	209.741	14.162
		12 terms	54.026	209.741	14.162

From Tables 3-5, shown in Appendix, the first three dimensionless critical buckling loads of the 2D-FGBs with SS, CC, and CF boundary conditions are presented for two different aspect ratios (L/h=5 and L/h=20), and a range of gradient indices in both directions (P_z and P_x). The first three critical buckling loads are seen to decrease for all sorts of boundary conditions as the gradient indices increase. It is found that the shear deformation effect increases in importance as the buckling mode number increases. The relative difference between the critical buckling loads with respect to aspect ratio change increases for CC beams as the buckling mode order increases [29].

Comparing the values of the critical buckling loads for aspect ratios of L/h = 5 and L/h = 20 for the suggested boundary conditions, it can be deduced that the CF beam has the lowest value while the CC beam has the largest value. Finally, the dimensionless critical buckling load is reduced by the gradient index variation in the x-direction more so than the gradient index variation in the z-direction.

The effects of gradient indices (px and pz) and aspect ratios on the dimensionless buckling stresses of the 2D-FGBs under various boundary conditions are shown in Figures 4 to 6. It has been found that the dimensionless critical buckling load decreases as gradient indices increase.

This results from a reduction in the stiffness of the beam [30]. It shows that the gradient index in the x direction has a bigger effect on the dimensionless critical buckling load than the gradient index in the z direction for all types of boundary conditions.
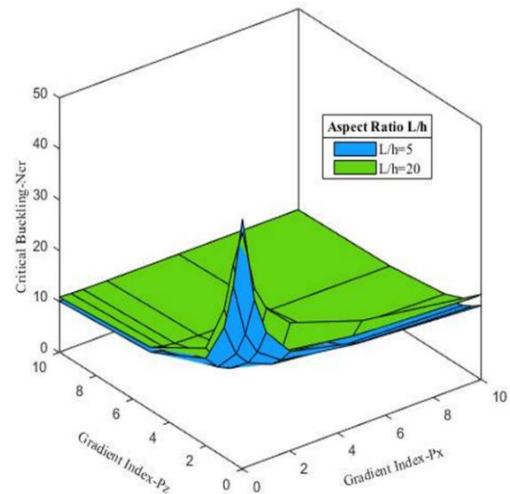
Fig. 4. Critical buckling (Ncr) of SS beam at various aspect ratios and gradient index
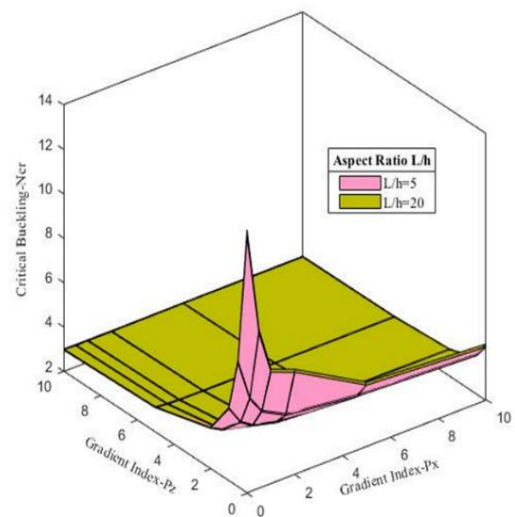
Fig. 5. Critical buckling (Ncr) of CF beam at various aspect ratios and gradient index
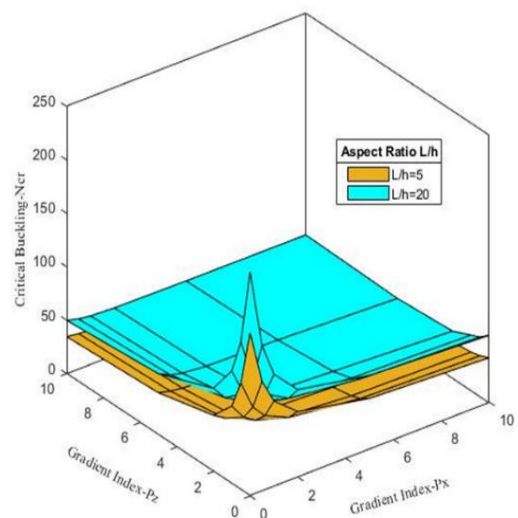
Fig. 6. Critical buckling (Ncr) of CC beam at various aspect ratios and gradient index

The influence of porosity pattern (even and uneven) on the critical buckling load is presented in Tables 6 to 8 and Figures 7 to 9. The critical buckling load for a pure ceramic FG beam is observed to be at its maximum value, and the buckling load decreases as the gradient index value increases because the metal constituent of the FG beam increases as the gradient index increases [23, 30].

On the other hand, as the FG beam goes from being perfect to imperfect, the critical buckling load declines noticeably with the high buckling modes. When it comes to porosity patterns, an uneven pattern is more noticeable than a uniform one in terms of buckling curves. This can be explained by the way that porosity is dispersed throughout the entire structure, with concentrated pores in the middle of the beam having a major impact on buckling response more so than evenly distributed pores [31]. As a result, while analyzing the stability of such structural components, the distribution profile of pores is a crucial factor in the buckling response of the FG beam.

Table 6. Influence of gradient exponents and porosity distribution on dimensionless critical buckling of a simply supported (SS) 2D FG beam at aspect ratio L/h=5

Px & Pz	Even Porosity				Uneven Porosity			
	0	0.1	0.2	0.3	0	0.1	0.2	0.3
0	49.0987	46.2213	43.3438	40.4664	49.0987	48.1533	47.2021	46.2449
0.5	30.036	27.4438	24.8864	22.3692	30.036	29.1784	28.3137	27.441
1	20.6701	18.0904	15.5585	13.0814	20.6701	19.8135	18.9472	18.0694
2	16.7171	14.07	11.4592	8.8354	16.7171	15.7872	14.8342	13.8512
5	13.2142	10.4455	7.7	4.5981	13.2142	12.2171	11.1895	10.1219
10	11.4151	8.5481	5.6932	2.7892	11.4151	10.3859	9.3216	8.2144

Table 7. Influence of gradient exponents and porosity distribution on dimensionless critical buckling of a clamped free (CF) 2D FG beam at the aspect ratio L/h=5

Px & Pz	Even Porosity				Uneven Porosity			
	0	0.1	0.2	0.3	0	0.1	0.2	0.3
0	13.5618	12.7885	12.0153	11.24198	13.5618	13.3208	13.0794	12.8374
0.5	5.747	5.4364	5.1259	4.8153	5.747	5.6502	5.5533	5.4561
1	4.0713	3.6412	3.2111	2.781	4.0713	3.9367	3.8015	3.6656
2	3.3054	3.0915	2.4749	2.0486	3.3054	3.1676	3.0274	2.884
5	2.9733	2.9117	2.3462	1.687	2.9733	2.9334	2.903	2.8725
10	2.9181	2.7511	2.0898	1.3764	2.9181	2.7939	2.6793	2.62

Table 8. Influence of gradient exponents and porosity distribution on dimensionless critical buckling of a clamped –clamped (CC) 2D FG beam at the aspect ratio L/h=5

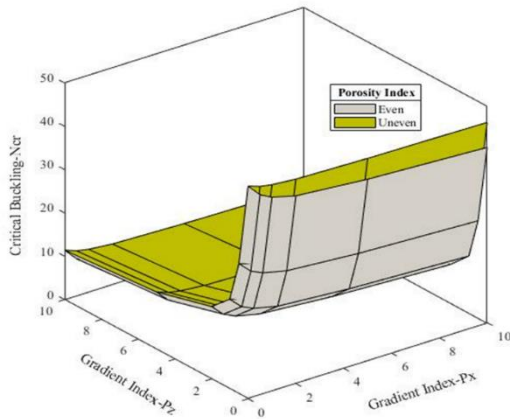| Px & Pz	Even Porosity				Uneven Porosity			
	0	0.1	0.2	0.3	0	0.1	0.2	0.3
0	152.6496	143.6405	134.6318	125.6231	152.6496	149.9487	147.247	144.544
0.5	80.0819	67.4412	56.5971	44.3822	80.0819	74.5723	71.3645	68.0884
1	50.5415	41.0822	30.1532	16.7305	50.5415	48.1873	44.9595	41.642
2	38.2772	31.0614	20.4039	8.5326	38.2772	38.0332	34.8157	31.4762
5	31.9311	24.8779	14.8718	3.989	31.9311	31.5725	28.5979	25.5229
10	30.1944	21.9149	12.5248	2.6324	30.1944	28.3847	25.6111	22.7969

Fig. 7. Critical buckling of SS beam with even porosity and uneven porosity at aspect ratio L/h=5
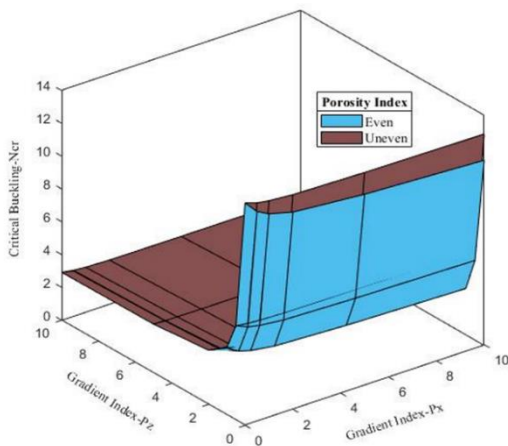

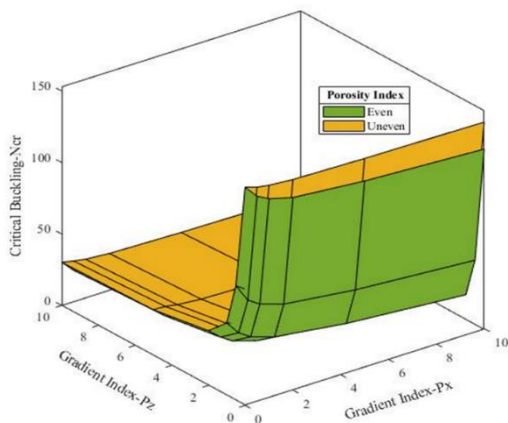**Fig. 8.** Critical buckling of CC beam with even porosity and uneven porosity at aspect ratio L/h=5

Fig. 9. Critical buckling of CC beam with even porosity and uneven porosity at aspect ratio L/h=5

4. Conclusions

This study shows the buckling behaviour of two-directional functionally graded beams with various boundary conditions. By using various gradient indices in both the axial and thickness directions, analytical polynomial series solutions are obtained for the boundary conditions Simply supported - Simply supported (SS), Clamped - clamped (CC), and Clamped-free (CF). It is studied how boundary conditions, gradient indices, and aspect ratios affect the circular buckling stress of 2D FG beams. The boundary conditions are met by the use of auxiliary functions. It is evident from the findings of the in-depth investigation that the gradient indices have a significant impact on the dimensionless buckling load of the 2D FG beams. However, the gradient index's impact in the z direction is more profound than its impact in the x direction.

By choosing appropriate gradient indexes, the buckling behaviour of the 2D FG beams can be managed to satisfy design requirements. The shear deformation effect on the critical buckling loads of the 2D FG beam reduces as the aspect ratio rises. The CC 2D FG beam is found to be significantly more susceptible to the shear deformation effect than the other 2D FG beam models.

The shear correction factor is not necessary since the third-order shear deformable beam theory that is used in this study to solve the buckling behavior of the two directional FGBs fulfills the zero traction boundary conditions on the top and bottom surfaces of the beam. It enables better buckling response prediction for the 2D FG beams. Higher-order shear deformation beam theories are required because the shear deformation effect is crucial, particularly for thick beams. Finally, the suggested theory effectively addresses the buckling behaviour of the 2D FG beams and yields accurate findings.

Nomenclature

FGM	Functionally graded materials
CC	Clamped - clamped
SS	Simply supported
CF	Clamped-free
CBT	Classical beam theory
TBT	Timoshenko beam theory
L	Length
B	Width
h	Thickness
Vf	Porous volume fraction
Px	Volume fraction through thickness
Pz	Volume fraction through length
α	Coefficient of porosity
E	Young's modulus
ρ	Mass density
U	Axial displacement
W	Transverse displacement
∅	Shear slope
F(z)	Shape function

Acknowledgments

Conflicts of Interest

The authors declares that there is no conflict of interest regarding the publication of this manuscript. In addition, the authors have entirely observed the ethical issues, including plagiarism, informed consent, misconduct, data fabrication and/or falsification, double publication and/or submission, and redundancy.

Appendix

Table 3. Influence of gradient exponents and aspect ratio on dimensionless critical buckling (Ncr) of a SS two directional FG beam, L/h=5 and L/h=20

Beam Theory		Px	L/h = 5 for Pz						L/h=20 for Pz					
			0	0.5	1	2	5	10	0	0.5	1	2	5	10
P R E S E N T	2 terms	0	58.43	40.49	34.68	28.30	21.20	17.31	63.65	44.65	39.64	32.62	26.60	19.57
	4 terms		49.12	32.69	25.40	19.68	16.45	14.59	53.77	35.26	27.08	21.33	18.10	16.72
	6 terms		49.10	32.37	25.09	19.57	16.15	14.55	53.74	35.04	27.06	21.22	17.99	16.41
	8 terms		49.10	32.37	25.09	19.57	16.15	14.55	53.74	35.04	27.06	21.22	17.99	16.41
	10 terms		49.10	32.37	25.09	19.57	16.15	14.55	53.74	35.04	27.06	21.22	17.99	16.41
	12 terms		49.10	32.37	25.09	19.57	16.15	14.55	53.74	35.04	27.06	21.22	17.99	16.41
P R E S E N T	2 terms	0.5	42.70	33.46	26.84	22.64	18.00	15.50	46.51	34.64	29.75	25.22	20.36	16.73
	4 terms		36.76	24.77	22.19	18.56	14.77	13.75	41.34	29.33	23.32	19.31	17.29	16.27
	6 terms		34.77	24.50	20.08	16.74	14.50	13.26	39.05	27.02	22.01	18.38	16.18	14.85
	8 terms		34.77	24.50	20.08	16.74	14.50	13.26	39.05	27.02	22.01	18.38	16.18	14.85
	10 terms		34.77	24.50	20.08	16.74	14.50	13.26	39.05	27.02	22.01	18.38	16.18	14.85
	12 terms		34.77	24.50	20.08	16.74	14.50	13.26	39.05	27.02	22.01	18.38	16.18	14.85
P R E S E T	2 terms	1	34.82	30.41	22.93	19.79	16.34	14.49	37.92	33.80	24.60	21.21	17.60	15.66
	4 terms		27.20	20.55	18.85	16.53	14.09	12.47	31.31	24.31	21.30	17.29	16.27	15.24
	6 terms		25.49	19.45	16.82	14.78	13.25	12.28	29.01	21.62	18.54	16.27	14.72	13.67
	8 terms		25.49	19.45	16.82	14.78	13.25	12.28	29.01	21.62	18.54	16.27	14.72	13.67
	10 terms		25.49	19.45	16.82	14.78	13.25	12.28	29.01	21.62	18.54	16.27	14.72	13.67
	12 terms		25.49	19.45	16.82	14.78	13.25	12.28	29.01	21.62	18.54	16.27	14.72	13.67
P R E S E N T	2 terms	2	26.94	23.46	19.01	16.93	14.65	13.43	29.33	3.65	20.45	18.20	15.81	14.53
	4 terms		18.18	16.18	14.17	13.16	12.14	11.12	21.34	18.34	16.33	14.71	14.10	13.27
	6 terms		17.13	14.58	13.44	12.51	11.67	11.08	19.15	16.05	14.72	13.70	12.86	12.22
	8 terms		17.13	14.58	13.44	12.51	11.67	11.08	19.15	16.05	14.72	13.70	12.86	12.22
	10 terms		17.13	14.58	13.44	12.51	11.67	11.08	19.15	16.05	14.72	13.70	12.86	12.22
	12 terms		17.13	14.58	13.44	12.51	11.67	11.08	19.15	16.05	14.72	13.70	12.86	12.22
P R E S E N T	2 terms	5	19.06	17.46	15.09	14.06	12.94	12.35	20.74	18.15	16.29	15.18	14.00	13.38
	4 terms		13.18	12.17	11.46	11.15	10.83	10.11	14.64	14.33	13.92	12.81	12.29	11.27
	6 terms		11.49	10.91	10.65	10.40	10.12	9.93	12.43	11.78	11.50	11.27	11.04	10.85
	8 terms		11.49	10.91	10.65	10.40	10.12	9.93	12.43	11.78	11.50	11.27	11.04	10.85
	10 terms		11.49	10.91	10.65	10.40	10.12	9.93	12.43	11.78	11.50	11.27	11.04	10.85
	12 terms		11.49	10.91	10.65	10.40	10.12	9.93	12.43	11.78	11.50	11.27	11.04	10.85
P R E S E N T	2 terms	10	15.48	13.41	13.31	12.76	12.16	11.85	17.83	15.59	14.41	13.80	13.18	12.85
	4 terms		11.15	10.75	10.34	10.12	9.91	9.68	13.31	12.71	12.30	11.89	11.27	10.74
	6 terms		10.09	9.93	9.84	9.76	9.65	9.58	10.85	10.69	10.62	10.56	10.50	10.45
	8 terms		10.09	9.93	9.84	9.76	9.65	9.58	10.85	10.69	10.62	10.56	10.50	10.45
	10 terms		10.09	9.93	9.84	9.76	9.65	9.58	10.85	10.69	10.62	10.56	10.50	10.45
	12 terms		10.09	9.93	9.84	9.76	9.65	9.58	10.85	10.69	10.62	10.56	10.50	10.45

Table 4. Influence of gradient exponents and aspect ratio on dimensionless critical buckling (Ncr) of
a CF two directional FG beam, L/h=5 and L/h=20

Beam Theory	Px	L/h=5				Pz		L/h=20				Pz	
		0	0.5	1	2	5	10	0	0.5	1	2	5	10
PRESENT													
2 terms	0	13.66	9.00	7.08	6.66	4.78	4.50	13.98	9.94	7.93	6.81	5.00	4.60
4 terms		13.56	9.00	7.04	6.63	4.78	4.43	13.91	9.43	7.33	6.79	4.95	4.55
6 terms		13.56	8.99	7.04	6.61	4.77	4.38	13.87	9.17	7.17	6.74	4.90	4.51
8 terms		13.56	8.99	7.04	6.61	4.77	4.38	13.87	9.17	7.17	6.74	4.90	4.51
10 terms		13.56	8.99	7.04	6.61	4.77	4.38	13.87	9.17	7.17	6.74	4.90	4.51
12 terms		13.56	8.99	7.04	6.61	4.77	4.38	13.87	9.17	7.17	6.74	4.90	4.51
PRESENT													
2 terms	0.5	8.56	6.38	5.43	4.72	4.01	3.73	8.75	6.70	5.56	4.82	4.10	3.82
4 terms		7.79	5.97	5.17	4.59	3.99	3.73	8.00	6.40	5.24	4.65	4.09	3.82
6 terms		7.59	5.75	4.97	4.39	3.99	3.72	7.70	5.83	5.04	4.47	4.08	3.81
8 terms		7.59	5.75	4.97	4.39	3.99	3.72	7.70	5.83	5.04	4.47	4.08	3.81
10 terms		7.59	5.75	4.97	4.39	3.99	3.72	7.70	5.83	5.04	4.47	4.08	3.81
12 terms		7.59	5.75	4.97	4.39	3.99	3.72	7.70	5.83	5.04	4.47	4.08	3.81
PRESET													
2 terms	1	7.02	4.59	4.51	4.19	3.69	3.42	7.17	4.76	4.61	4.28	3.77	3.50
4 terms		5.49	4.46	4.17	3.94	3.62	3.40	5.76	4.54	4.34	4.03	3.67	3.47
6 terms		5.25	4.43	4.07	3.79	3.56	3.39	5.31	4.48	4.12	3.85	3.63	3.47
8 terms		5.25	4.43	4.07	3.79	3.56	3.39	5.31	4.48	4.12	3.85	3.63	3.47
10 terms		5.25	4.43	4.07	3.79	3.56	3.39	5.31	4.48	4.12	3.85	3.63	3.47
12 terms		5.25	4.43	4.07	3.79	3.56	3.39	5.31	4.48	4.12	3.85	3.63	3.47
PRESENT													
2 terms	2	6.01	4.49	4.23	3.84	3.47	3.28	6.14	4.71	4.33	3.93	3.55	3.35
4 terms		4.37	3.97	3.83	3.65	3.27	3.13	4.51	4.01	3.91	3.76	3.29	3.22
6 terms		3.83	3.54	3.41	3.30	3.20	3.12	3.87	3.58	3.46	3.35	3.26	3.19
8terms		3.83	3.54	3.41	3.30	3.20	3.12	3.87	3.58	3.46	3.35	3.26	3.19
10 terms		3.83	3.54	3.41	3.30	3.20	3.12	3.87	3.58	3.46	3.35	3.26	3.19
12 terms		3.83	3.54	3.41	3.30	3.20	3.12	3.87	3.58	3.46	3.35	3.26	3.19
PRESENT													
2 terms	5	5.06	3.98	3.83	3.56	3.30	3.17	5.17	4.10	3.91	3.63	3.37	3.24
4 terms		3.86	3.37	3.20	3.19	3.18	3.07	4.31	3.42	3.27	3.22	3.20	3.12
6 terms		3.11	3.05	3.02	3.00	2.97	2.95	3.15	3.09	3.07	3.05	3.03	3.01
8 terms		3.11	3.05	3.02	3.00	2.97	2.95	3.15	3.09	3.07	3.05	3.03	3.01
10 terms		3.11	3.05	3.02	3.00	2.97	2.95	3.15	3.09	3.07	3.05	3.03	3.01
12 terms		3.11	3.05	3.02	3.00	2.97	2.95	3.15	3.09	3.07	3.05	3.03	3.01
PRESENT													
2 terms	10	4.37	3.64	3.54	3.36	3.19	3.10	4.47	3.76	3.62	3.43	3.26	3.17
4 terms		3.79	3.32	3.17	3.17	3.06	2.96	3.96	3.39	3.28	3.22	3.09	3.01
6 terms		2.96	2.95	2.94	2.93	2.92	2.92	3.01	2.99	2.99	2.98	2.98	2.97
8 terms		2.96	2.95	2.94	2.93	2.92	2.92	3.01	2.99	2.99	2.98	2.98	2.97
10 terms		2.96	2.95	2.94	2.93	2.92	2.92	3.01	2.99	2.99	2.98	2.98	2.97
12 terms		2.96	2.95	2.94	2.93	2.92	2.92	3.01	2.99	2.99	2.98	2.98	2.97

Table 5. Influence of gradient exponents and aspect ratio on dimensionless critical buckling (Ncr) of
a CC two directional FG beam, L/h=5 and L/h=20

Beam Theory	Px	L/h=5			Pz			L/h=20			Pz		
		0	0.5	1	2	5	10	0	0.5	1	2	5	10
P R E S E N T	2 terms	159.44	123.05	100.16	75.81	62.37	56.17	224.45	145.87	121.30	92.53	76.11	68.55
	4 terms	154.54	109.73	89.28	67.68	55.62	50.02	212.60	136.85	112.10	84.90	69.76	62.77
	6 terms	152.65	102.77	79.99	61.38	47.39	41.49	209.46	136.37	105.07	81.97	68.83	62.50
	8 terms	152.65	102.77	79.99	61.38	47.39	41.49	209.46	136.37	105.07	81.97	68.83	62.50
	10 terms	152.65	102.77	79.99	61.38	47.39	41.49	209.46	136.37	105.07	81.97	68.83	62.50
	12 terms	152.65	102.77	79.99	61.38	47.39	41.49	209.46	136.37	105.07	81.97	68.83	62.50
P R E S E N T	2 terms	128.39	93.76	75.80	62.87	54.63	49.89	152.04	115.78	92.51	76.72	66.66	60.86
	4 terms	106.55	81.74	67.34	55.99	48.70	44.52	142.23	107.85	84.52	70.25	61.11	55.85
	6 terms	99.75	73.08	60.69	50.19	41.57	37.56	138.50	98.19	81.00	68.13	59.92	55.13
	8 terms	99.75	73.08	60.69	50.19	41.57	37.56	138.50	98.19	81.00	68.13	59.92	55.13
	10 terms	99.75	73.08	60.69	50.19	41.57	37.56	138.50	98.19	81.00	68.13	59.92	55.13
	12 terms	99.75	73.08	60.69	50.19	41.57	37.56	138.50	98.19	81.00	68.13	59.92	55.13
P R E S E T	2 terms	101.92	81.81	66.64	57.48	51.14	47.27	123.28	93.90	80.09	68.94	60.97	57.16
	4 terms	78.92	64.66	59.38	51.25	45.63	42.19	113.57	87.89	74.45	64.26	57.22	52.91
	6 terms	72.60	57.87	50.54	43.99	38.27	35.40	105.47	80.31	69.25	60.71	54.85	51.19
	8 terms	72.60	57.87	50.54	43.99	38.27	35.40	105.47	80.31	69.25	60.71	54.85	51.19
	10 terms	72.60	57.87	50.54	43.99	38.27	35.40	105.47	80.31	69.25	60.71	54.85	51.19
	12 terms	72.60	57.87	50.54	43.99	38.27	35.40	105.47	80.31	69.25	60.71	54.85	51.19
P R E S E N T	2 terms	65.84	53.73	47.93	42.53	38.56	36.26	84.44	71.85	67.07	57.54	53.00	46.47
	4 terms	52.59	45.49	41.77	38.28	35.01	33.21	77.87	64.49	58.33	53.37	49.71	43.50
	6 terms	52.59	45.49	41.77	38.28	35.01	33.21	77.87	64.49	58.33	53.37	49.71	43.50
	8 terms	52.59	45.49	41.77	38.28	35.01	33.21	77.87	64.49	58.33	53.37	49.71	43.50
	10 terms	52.59	45.49	41.77	38.28	35.01	33.21	77.87	64.49	58.33	53.37	49.71	43.50
	12 terms	52.59	45.49	41.77	38.28	35.01	33.21	77.87	64.49	58.33	53.37	49.71	43.50
P R E S E N T	2 terms	70.08	57.76	52.26	48.19	44.99	42.83	72.02	63.73	58.76	54.86	50.79	45.23
	4 terms	51.98	41.84	38.48	35.30	32.78	32.14	65.21	56.65	52.64	49.84	47.03	41.54
	6 terms	39.38	36.46	34.88	33.37	31.93	31.08	57.16	51.59	48.86	46.57	44.78	39.75
	8 terms	39.38	36.46	34.88	33.37	31.93	31.08	57.16	51.59	48.86	46.57	44.78	39.75
	10 terms	39.38	36.46	34.88	33.37	31.93	31.08	57.16	51.59	48.86	46.57	44.78	39.75
	12 terms	39.38	36.46	34.88	33.37	31.93	31.08	57.16	51.59	48.86	46.57	44.78	39.75
P R E S E N T	2 terms	59.26	49.61	46.84	44.47	42.48	41.04	59.91	54.90	52.10	48.86	45.82	43.77
	4 terms	43.03	38.76	35.56	33.48	31.75	30.62	54.24	50.09	47.95	45.54	44.02	43.36
	6 terms	34.54	33.00	32.17	31.40	30.68	30.20	49.87	46.79	45.24	43.91	42.81	41.97
	8 terms	34.54	33.00	32.17	31.40	30.68	30.20	49.87	46.79	45.24	43.91	42.81	41.97
	10 terms	34.54	33.00	32.17	31.40	30.68	30.20	49.87	46.79	45.24	43.91	42.81	41.97
	12 terms	34.54	33.00	32.17	31.40	30.68	30.20	49.87	46.79	45.24	43.91	42.81	41.97

Note: Px values by block: 0, 0.5, 1, 2, 5, 10

References

[1] Miyamoto, Y., Kaysser, W.A., Rabin, B.H., Kawasaki, A. and Ford, R.G., 1999. Processing and fabrication. In Functionally Graded Materials (pp. 161-245). Springer, Boston, MA.

[2] Chawla, N. and Chawla, K.K., 2013. Processing. In Metal Matrix Composites (pp. 55-97). Springer, New York, NY.

[3] Mortensen, A. and Suresh, S., 1998. Fundamentals of Functionally Graded Materials: Processing and Thermomechanical Behaviour of Graded Metals and Metal-ceramic Composites (Book. Maney Publishing.

[4] Anandrao, K.S., Gupta, R.K., Ramchandran, P. and Rao, G.V., 2010. Thermal post-buckling analysis of uniform slender functionally graded material beams. Structural engineering and mechanics: An international journal, 36(5), pp.545-560.

[5] Aydogdu, M. and Taskin, V., 2007. Free vibration analysis of functionally graded beams with simply supported edges. Materials & design, 28(5), pp.1651-1656.

[6] Singh, K.V. and Li, G., 2009. Buckling of functionally graded and elastically restrained non-uniform columns. Composites Part B: Engineering, 40(5), pp.393-403.

[7] Zhen, W. and Wanji, C., 2006. A higher-order theory and refined three-node triangular element for functionally graded plates. European Journal of Mechanics-A/Solids, 25(3), pp.447-463.

[8] Thai, H.T. and Vo, T.P., 2012. Bending and free vibration of functionally graded beams using various higher-order shear deformation beam theories. International journal of mechanical sciences, 62(1), pp.57-66.

[9] Nguyen, T.K., Vo, T.P. and Thai, H.T., 2013. Static and free vibration of axially loaded functionally graded beams based on the first-order shear deformation theory. Composites Part B: Engineering, 55, pp.147-157.

[10] Ebrahimi, F. and Barati, M.R., 2016. A nonlocal higher-order shear deformation beam theory for vibration analysis of size-dependent functionally graded nanobeams. Arabian Journal for Science and Engineering, 41(5), pp.1679-1690.

[11] Kim, J., Żur, K.K. and Reddy, J.N., 2019. Bending, free vibration, and buckling of modified couples stress-based functionally graded porous micro-plates. Composite Structures, 209, pp.879-888.

[12] Hebbar, N., Hebbar, I., Ouinas, D. and Bourada, M., 2020. Numerical modeling of bending, buckling, and vibration of functionally graded beams by using a higher-order shear deformation theory. Frattura ed Integrità Strutturale, 14(52), pp.230-246.

[13] Nejad, M.Z., Hadi, A. and Rastgoo, A., 2016. Buckling analysis of arbitrary two-directional functionally graded Euler–Bernoulli nano-beams based on nonlocal elasticity theory. International Journal of Engineering Science, 103, pp.1-10.

[14] Şimşek, M., 2015. Bi-directional functionally graded materials (BDFGMs) for free and forced vibration of Timoshenko beams with various boundary conditions. Composite Structures, 133, pp.968-978.

[15] Sayyad, A.S. and Ghugal, Y.M., 2017. Bending, buckling and free vibration of laminated composite and sandwich beams: A critical review of literature. Composite Structures, 171, pp.486-504.

[16] Ramu, I. and Mohanty, S.C., 2014. Buckling analysis of rectangular functionally graded material plates under uniaxial and biaxial compression load. Procedia Engineering, 86, pp.748-757.

[17] Trinh, M.C., Mukhopadhyay, T. and Kim, S.E., 2020. A semi-analytical stochastic buckling quantification of porous functionally graded plates. Aerospace Science and Technology, 105, p.105928.

[18] Adhikari, B., Dash, P. and Singh, B.N., 2020. Buckling analysis of porous FGM sandwich plates under various types nonuniform edge compression based on higher order shear deformation theory. Composite Structures, 251, p.112597.

[19] Magnucki, K. and Stasiewicz, P., 2004. Elastic buckling of a porous beam. Journal of Theoretical and Applied Mechanics, 42(4), pp.859-868.

[20] Magnucka-Blandzi, E. and Magnucki, K., 2007. Effective design of a sandwich beam with a metal foam core. Thin-Walled Structures, 45(4), pp.432-438.

[21] Galeban1a, M.R., Mojahedin, A., Taghavi, Y. and Jabbari, M., 2016. Free vibration of functionally graded thin beams made of saturated porous materials. Steel and Composite Structures, 21(5), pp.999-1016.

[22] Babaei, M., Asemi, K. and Safarpour, P., 2019. Natural frequency and dynamic analyses of functionally graded saturated porous beam resting on viscoelastic foundation based on higher order beam theory. Journal of Solid Mechanics, 11(3), pp.615-634.

[23] Mojahedin, A., Jabbari, M. and Rabczuk, T., 2018. Thermoelastic analysis of functionally

graded porous beam. Journal of Thermal Stresses, 41(8), pp.937-950.

[24] Hung, T.Q., Duc, D.M. and Tu, T.M., 2022. Static Behavior of Functionally Graded Sandwich Beam with Fluid-Infiltrated Porous Core. In Modern Mechanics and Applications (pp. 691-706). Springer, Singapore.

[25] Nathi, V.K., 2022. Buckling analysis of 2D functionally graded porous beams using novel higher order theory. Journal of Computational Applied Mechanics, 53(3), pp.393-413.

[26] Zhang, D.G. and Zhou, Y.H., 2008. A theoretical analysis of FGM thin plates based on physical neutral surface. Computational Materials Science, 44(2), pp.716-720.

[27] Karamanlı, A., 2018. Analytical solutions for buckling behavior of two directional functionally graded beams using a third order shear deformable beam theory. Academic Platform-Journal of Engineering and Science, 6(2), pp.164-178.

[28] Nguyen, T.K., Nguyen, T.T.P., Vo, T.P. and Thai, H.T., 2015. Vibration and buckling analysis of functionally graded sandwich beams by a new higher-order shear deformation theory. Composites Part B: Engineering, 76, pp.273-285.

[29] Nemat-Alla, M., 2003. Reduction of thermal stresses by developing two-dimensional functionally graded materials. International journal of solids and structures, 40(26), pp.7339-7356.

[30] Karamanlı, A., 2017. Elastostatic analysis of two-directional functionally graded beams using various beam theories and Symmetric Smoothed Particle Hydrodynamics method. Composite Structures, 160, pp.653-669.

[31] Van Do, T., Nguyen, D.K., Duc, N.D., Doan, D.H. and Bui, T.Q., 2017. Analysis of bi-directional functionally graded plates by FEM and a new third-order shear deformation plate theory. Thin-Walled Structures, 119, pp.687-699.